

## Real-Time Estimation of SAG Mill Charge Characteristics for Process Optimization

---

\*P. Toor<sup>1</sup>, W. Valery<sup>1</sup>, S. Morrell<sup>2</sup>, K. Duffy<sup>1</sup>

<sup>1</sup>Hatch  
61 Petrie Terrace  
Brisbane, QLD, 4000, Australia

<sup>2</sup>SMC Testing  
Kenmore Hills, QLD, 4069, Australia

(\*Corresponding author: [paul.toor@hatch.com](mailto:paul.toor@hatch.com))

### Abstract

---

Control of the total charge and the ball charge volume is vital to the optimum performance of semi-autogenous grinding (SAG) mills to maximise throughput and energy efficiency. However, neither of these parameters can be directly measured online. Where they are installed, load cells measure the mill and charge total mass. Where load cells are not installed, the total mass can be inferred from bearing pressure. The charge mass is then estimated by subtracting the mass of the mill shell plus lifters and liners; but, the liner mass changes with wear and mill relines. However, when combined with an accurate SAG mill power-draw model, total charge volume and ball load can be estimated with reasonable accuracy.

The Morrell C-model is generally regarded as one of the most accurate tumbling mill power-draw models and is ideally suited for this application of estimating fill levels of the SAG mill in real time. This paper presents three methods using the Morrell C-model to estimate total and ball charge volumes for SAG mills, depending on the data and measurements available. The methodologies outlined all allow analysis of real-time data and large data sets spanning months and years of operation, thus facilitating identification of optimum operating conditions and aiding in early detection, trouble-shooting, and rectifying poor mill performance. Several case studies are provided to demonstrate the application and accuracy of the results derived from the proposed methodologies.

### Keywords

---

SAG mill, power modelling, comminution, optimization



## Introduction

Semi-autogenous grinding (SAG) mill key performance indicators (KPI), such as throughput, specific-energy consumption, and product size, are sensitive to the total volumetric charge (mill filling) and the ball charge. Operating with low mill filling can reduce energy efficiency due to excess steel-to-steel contact, be it ball on ball or ball on liner. This can also cause lifter–liner failure and significantly reduce mill liner service life. Conversely, if the charge volume is too high throughput can decrease due to the excessive rock load dampening the grinding action.

The charge volume and throughput relationship varies from circuit to circuit, and throughput does not necessarily follow power draw. It has a maximum at a particular charge volume that also varies with other operating conditions, such as feed-size distribution, ball filling, and lifter–liner configuration (Figure 1 and Figure 2). Figure 1 shows the throughput and charge-volume relationship using measured data for three operations. Figure 2 shows the throughput versus SAG mill load for two different liner designs and operating loads, and the power draw versus SAG mill load for the Cadia SAG mill (Hart et al., 2001). Both show how the throughput and mill-charge relationship vary for different operations and conditions, and the value of measuring charge volume to maximise throughput.

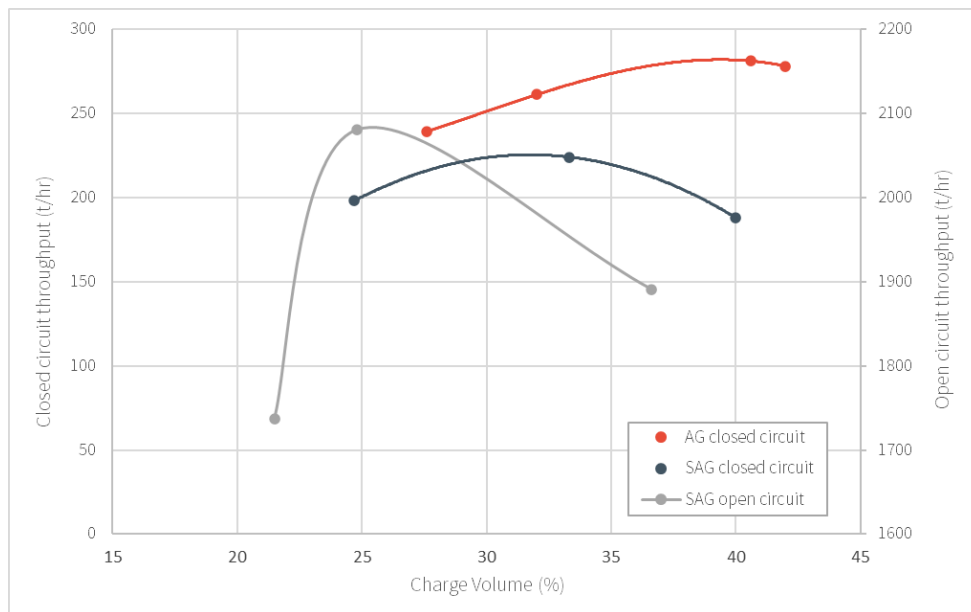


Figure 1—Mill filling—throughput response for a variety of circuit configurations

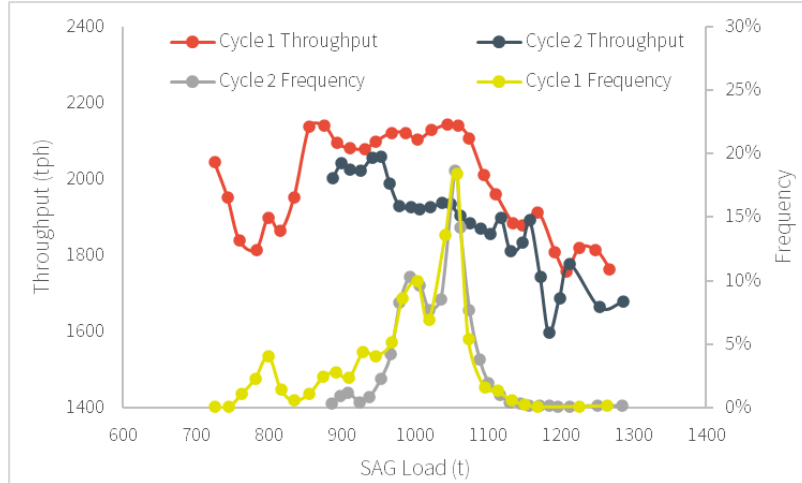


Figure 2—Mill filling—throughput response for a variety of circuit configurations (after Hart et al., 2001)

Mill charge volume cannot be measured directly due to the aggressive mill environment. Instead, mill load (weight) is reported, and this is either based on the output from a load cell installed under the feed or discharge end of the mill or inferred from bearing pressure. Thus, the mill load is a combined measurement of mill weight, liner weight, and total charge weight (rock and grinding media). The inclusion of liner weight is problematic due to mass loss over the liner life due to wear. Another complication is the differential densities of grinding media and ore; a reported mill load weight can correspond to a wide range of mill volumetric charge (with differing proportions of media to ore).

Considering the impact of total mill charge on SAG mill performance, the ability to infer its value from the available instrumentation is highly desirable. This would allow mill charge to be tracked at high resolution from process historian data rather than only from physical mill inspections, which are generally many months apart.

## Mill Power-Draw Modelling

Mill power-draw models aim to estimate how much power will be consumed by a particular mill geometry and operating configuration. These models are typically used for mill design and grinding circuit modelling (for optimization purposes). However, they could also be used to infer mill-charge volume, and there are many different power models that could be used for this purpose. The Morrell C-model is widely accepted to be the most accurate power model for tumbling mills. Therefore, we selected this model for determining key milling parameters.

The Morrell C-model was initially calibrated, and its validity tested, using 82 data sets covering a wide range of design and operating parameters for ball, SAG, and fully autogenous grinding (AG) mills (Morrell, 1996a, 1996b). The overall model accuracy was shown to be  $\pm 9.8\%$  at the 95% confidence level. Additional validation testing was conducted with independent data (i.e., different data than those used for calibration), and all observed data fell within the 95% confidence interval of the Morrell C-model predictions (Morrell, 2003). Doll (2013) confirms the Morrell C-model to be the most accurate using a comparison of three different power models (Austin, Loveday/Barratt, and Morrell C-model) using a much smaller data set—25 surveys from seven different operations.

Additionally, the Morrell C-model is a generalised tumbling mill model. Therefore, this model (and the associated approaches to charge estimation presented in this paper) can be applied to ball, SAG and AG mills, and the calculations cover grate and overflow discharge mills.

Several other Morrell power models and energy calculations should not be confused with the Morrell C-model used in this paper, including the following:

- Morrell energy–size relationships are well known and widely applied to estimate comminution circuits' specific energy, including AG, SAG, ball, and rod mills, and crushers and high-pressure grinding rolls (HPGR). Energy–size relationships can be used to assess the energy utilisation and efficiency of existing circuits and can also be used in conjunction with power models (such as the Morrell C-model) to arrive at the correct choice of equipment when designing a comminution circuit. These equations have been adopted by the Global Mining Guidelines Group (GMG) (GMG Group, 2021).
- The Morrell D-model uses a more sophisticated treatment of charge dynamics than the Morrell Continuum (or simply C) model; it was the precursor to the C-model. The total charge is subdivided into discrete layers (hence D-model) (or shells), and the potential and kinetic energy for each is calculated separately, then summed for total power draw. By contrast, the Morrell C-model treats the charge as a single shape comprising a continuum of layers (Figure 3). Therefore, the mathematics for the C-model are much simpler, without sacrificing too much accuracy, and more suitable for back-calculating mill charge from large and real-time data sets.
- The Morrell E-model is a simpler empirical model based on the C-model (Morrell, 1996b).

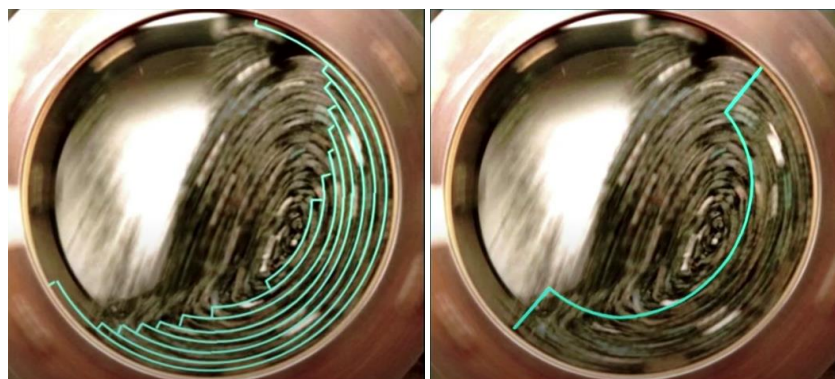


Figure 3—Visual representation of Morrell D-model (left) and C-model (right) (after Morrell, n.d.)

The Morrell C-model was selected for the purpose of estimating SAG mill charge, as it provides good accuracy using input data typically available in industrial operations, with equations that allow back-calculating mill charge.

## BRIEF INTRODUCTION TO MORRELL C-MODEL

The energy consumption (power draw) in a tumbling mill results from charge rotation. Therefore, accurate power modelling requires describing the charge dynamics.

The C model developed by Morrell at the JKMRRC as part of his PhD thesis (Morrell, 1993) is based on the motion of the grinding charge and considers this as a continuum. The model estimates the rate at which the mill shell imparts potential and kinetic energy to the charge, based on describing the charge shape and motion (Morrell, 1996a).

The C-model achieves this by first determining the geometry and velocity of the mill charge. The mill charge is assumed to comprise a continuum of concentric layers when the mill is operating. The power associated with the charge motion is estimated by using a mathematical description of the charge shape and position, and the particle velocities within it. In addition, energy is consumed due to inefficiencies in the motor and drive train, and heat loss due to friction, attrition and abrasion breakage, and grinding media rotation. Therefore, the overall model for gross power ( $P_{gross}$ ) is expressed as:

$$P_{gross} = P_{no-load} + k \times (P_{charge\ motion}) \quad (1)$$

The no-load power ( $P_{no-load}$ ) is the power input to the motor when the mill is empty; it is used to estimate motor and drive train inefficiencies. An empirical calculation of no-load power is provided in Morrell (1996a). The  $k$  factor is a lumped parameter that accounts for heat loss, energy consumed by attrition and abrasion breakage, measurement inaccuracies, and other assumptions. The  $k$  factor was calibrated to be 1.26 using 82 data sets (Morrell, 1996a, 1996b) and validated with additional independent data. The power associated with the charge motion ( $P_{charge\ motion}$ ) is calculated from the geometry and charge movement (velocity of the charge). The required input data for this calculation includes design and operating parameters of the mill and constants as follows:

#### Design and Operating Data:

- D Diameter inside liners (metres [m])
- L Belly length inside liners (m)
- D<sub>t</sub> Trunnion diameter inside liners (m)  
Discharge mechanism (grate or overflow)
- N<sub>m</sub> Mill rotational speed (revolutions per second [rps])
- φ Fraction of critical speed (fraction)
- ρ<sub>o</sub> Ore specific gravity of ore (tonnes per cubic metre [t/m<sup>3</sup>])
- ρ<sub>B</sub> Ball specific gravity (t/m<sup>3</sup>)
- J<sub>t</sub> Total fractional mill filling of cylindrical section (fraction)
- J<sub>B</sub> Ball fractional mill filling of cylindrical section (fraction)
- S Solids content of discharge slurry (fraction by volume)
- U Fraction of grinding media voidage occupied by slurry (fraction)
- E Fractional porosity of charge (fraction).

In the absence of data for E, S, and U, values of 0.4, 0.5, and 1, respectively, can be assumed (Morrell, 1996a).

#### Constants:

- g Acceleration due to gravity = 9.814 m/s/s
- k Morrell C-model calibration factor = 1.26

Tumbling mills consist of a cylindrical centre section and conical ends, and particularly for those with large diameter-to-length ratios, the geometry (and associated charge motion) of both sections must be considered to determine the overall charge-motion power draw. Therefore, there are two principal charge-motion power-draw equations, one for the cylindrical section ( $P_t$ ) and another for the conical section ( $P_c$ ) (Equations 2 and 3, respectively). The overall charge-motion power ( $P_{charge\ motion}$ ) is the sum of these (Equation 4).

Charge-motion power draw of cylindrical section ( $P_t$ ):

$$P_t = \frac{\pi g L d N_m r_m}{3(r_m - z r_i)} [2r_m^3 - 3z r_m^2 r_i + r_i^3 (3z - 2)] \times [\rho_c (\sin \theta_S - \sin \theta_T) + \rho_p (\sin \theta_T - \sin \theta_{TO})] + L \rho_c \left( \frac{N_m r_m \pi}{(r_m - z r_i)} \right)^3 [(r_m - z r_i)^4 - r_i^4 (z - 1)^4] \quad (2)$$

Charge-motion power draw of conical section ( $P_c$ ):

$$P_c = \frac{\pi L d g N_m}{3(r_m - r_t)} \left\{ (r_m^4 - 4r_m r_i^3 + 3r_i^4) \times [\rho_c (\sin \theta_S - \sin \theta_T) + \rho_p (\sin \theta_T - \sin \theta_{TO})] \right\} + \left( \frac{2\pi^3 N_m^3 L_d \rho_c}{5(r_m - r_t)} \right) (r_m^5 - 5r_m r_i^4 + 4r_i^5) \quad (3)$$

Total motion power draw:

$$P_{charge\ motion} = P_t + P_c \quad (4)$$

Where (in addition to the input variables already listed above):

$r_m$  = Mill radius (m)

$z = (1 - J_t)^{0.4532}$  (intermediate calculation required to describe the velocity profile using rotational rate)

$r_i$  = Radial location of inner surface of charge (m)

$\rho_c$  = Charge specific gravity (t/m<sup>3</sup>)

$\rho_p$  = Discharge pulp specific gravity (t/m<sup>3</sup>)

$\theta_S$  = Shoulder angle (radians)

$\theta_T$  = Toe angle (radians)

$\theta_{TO}$  = Slurry toe angle (radians)

$L_d$  = Cone-end length (m)

$r_t$  = Discharge trunnion radius (m).

These additional variables must be calculated before the charge-motion power equations can be computed. Some are simple, such as mill radius. However, others are more complex, including the charge's shoulder and toe angles, inner surface radius, and density. Nevertheless, all can be calculated from the input data listed previously, as Morrell (1996a) described. For clarity, Figure 4 contains schematic diagrams of a mill showing key measurements.

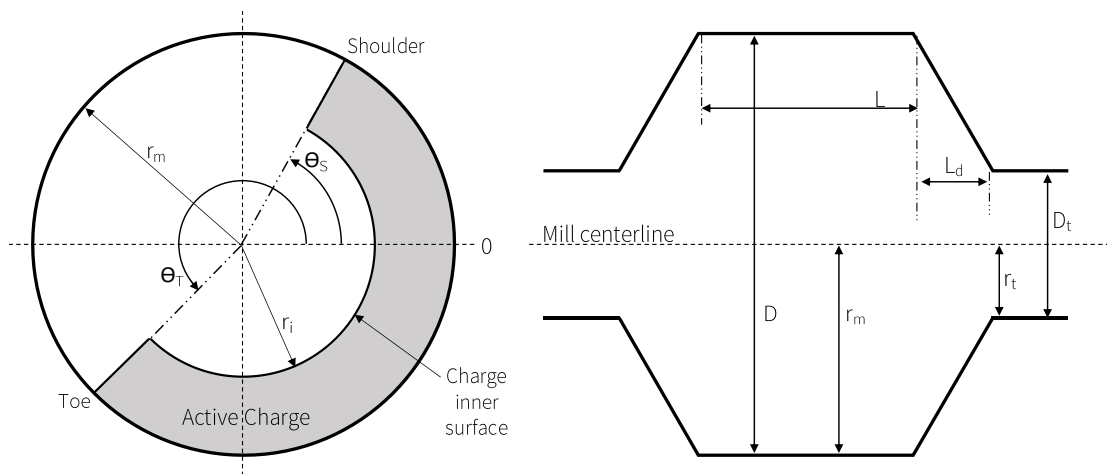


Figure 4—Schematic of mill showing key measurements

The Morrell C-model contains over 20 equations and sub-equations; it is not practical to repeat them here. However, it is reasonably straightforward to input and link these calculations in a Microsoft Excel spreadsheet. Full details of the model and its development can be found in Napier-Munn et al. (1996); it is also well described with all equations and a worked example in Morrell (1996a).

The Morrell C-model is commonly used for mill design and for evaluating and optimizing mill performance by predicting how much power is consumed for a particular mill geometry and operating conditions. It is the tumbling mill power model used in the JKSimMet modelling and simulation package. For circuit design, the Morrell C-model is used in conjunction with energy–size relationships to ensure selecting appropriately sized AG, SAG, and ball mills. In terms of optimizing existing circuits, an operating mill that draws power similar to that predicted by the model is generally performing well, while a lower power draw potentially indicates an issue and scope for improvement. In this paper, we consider the model use to determine total volumetric charge (mill filling,  $J_T$ ) for optimization and troubleshooting.

### Morrell C-Model Used to Estimate Mill Filling

The Morrell C-model has proven to be an accurate power model for ball, SAG, and AG mills. As mill filling is an model input parameter, it should be possible to back-calculate this if all other parameters and the power draw are known. This was demonstrated as early as 2001 through incorporation in what was called at the time JK SAG Charge; it was successfully applied at Mount Isa Mines and Ernest Henry (Strohmayer & Valery, 2001; Lawson et al., 2001).

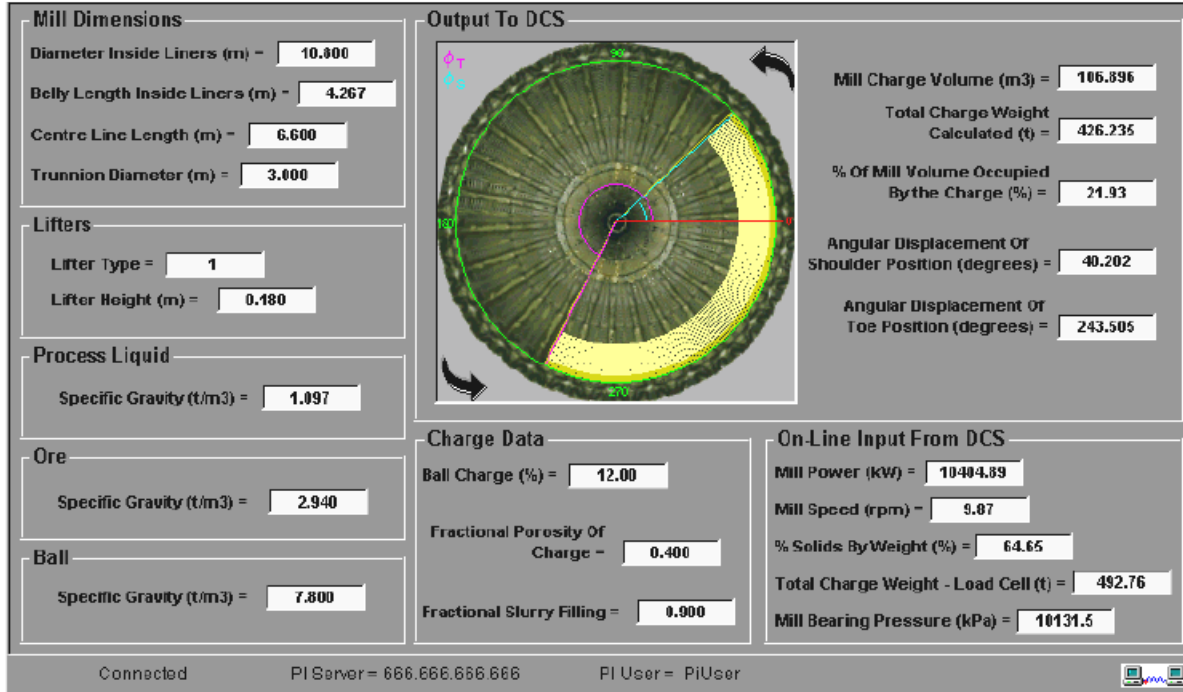


Figure 5—JK SAG charge interface window

Due to the interrelated equations and sub-equations, there is no simple algebraic solution for total mill filling ( $J_T$ ), even when all other parameters are known. An iterative approach is required to calculate either total mill filling or ball charge for a given mill power-draw. This makes analysis of large data sets difficult, and results in the underuse of a potentially powerful tool for SAG mill operation and optimization. Typically, plant metallurgists will only use the Morrell C-model to calculate the ball charge from a crash-stop inspection, which is only conducted periodically (but infrequently) due to the significant production disruption.

Visual Basic for Applications (VBA) programming in Excel can be used to perform the iterative calculation of mill filling using power-modelling equations to work with large data sets such as process historian data. The calculation of mill filling (aided by VBA) can be carried out for both real time prediction or conducted on historical data sets. Interrogation of historical data facilitates the identification of optimum operating conditions, whilst real time analysis enables early detection, trouble shooting and rectification of instances of poor mill performance.

In SAG mills, the mill filling consists of the rock charge and grinding media, and power models cannot determine the proportion of grinding media in the charge. Therefore, a range of total mill fillings is possible at different ball-charge levels. Three methods for applying the Morrell C-model to determine total mill filling are described, each depending on what data are available to determine the ball-charge level. These are as follows:

- Known or modelled ball charge
- Toe angel detection
- Laser scanning of mill liners and wear modelling.

These methods are described in the following sections, using case study examples.



## **CASE STUDY 1: DETERMINING MILL CHARGE WITH KNOWN OR MODELLED BALL CHARGE**

The simplest application of the Morrell C-model to calculate total mill filling is when the ball charge is known. In ball mills it is common practice for operators to charge balls to a power set-point. As ball mills often have very stable power draw, in some cases it may be assumed that the ball charge remains relatively constant. Therefore, once ball filling has been measured for the power set-point (this would require crash-stop and grind-out), this value of ball filling could be assumed at that power draw. However, care should be taken using this assumption, particularly if there are significant changes in feed ore characteristics or other operating conditions.

Alternatively, for SAG mills where power draw is less stable, the ball charge could be modelled using a ball charge mass balance. An initial grind-out and ball charge measurement is required, then the ball charge can be adjusted according to the measured tonnes of balls added and the typical grinding media consumption rate determined from historical data.

In this case study of a 32-foot (ft) variable-speed SAG mill, the ball charge was known to be relatively constant across a six-month period, which coincided with a shell lifter–liner life cycle. If ball charge is known, calculating the mill filling is relatively simple for a single data point using Excel Solver. The mill filling value is adjusted until the Morrell C-model-calculated power-draw matches the measured power draw.

VBA programming in Excel can be used to conduct this iterative calculation quickly for a larger data set. In this case study, the process historian data was analysed for the same six-month period using the daily averages for mill power, speed, and slurry density. The VBA code achieved the calculations for the 169 data points in a matter of seconds. This was achieved using “Do Until” and “Loop” VBA commands and the goal seek function in Excel, which can be coded using VBA or recorded using the macro record function in Excel.

The results of the analysis are shown in Figure 6. The process historian values for mill power, mill speed, and mill weight are plotted alongside the mill charge calculated using the Morrell C-model. Three mill charge measurements were taken during the six-month period (also shown in Figure 6) and these align closely with the calculated mill charges. This demonstrates that the Morrell C-model can be used to calculate mill charge when the ball charge is known.

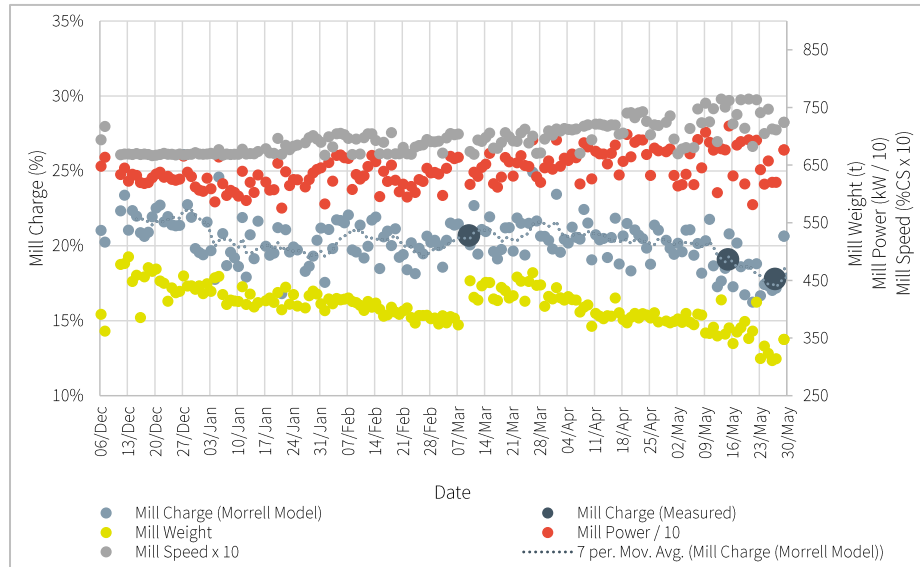


Figure 6—Calculated and measured mill charge, mill speed, and mill weight (ball charge known)

Figure 6 shows that there is a significant difference in the mill weight and calculated mill filling trends. This reflects the significant impact of changing liner weight due to wear and mill relines, and demonstrates that mill weight needs to be constantly adjusted if it is to be used to infer mill filling for process control and optimization. Calculating mill charge using power modelling provides a more consistent measurement for process performance optimization, assuming ball charge is known or modelled.

## CASE STUDY 2: DETERMINING MILL CHARGE WITH TOE POSITION MEASUREMENT

Mill-mounted sensors to measure the toe position and direct impact of grinding media on the shell liners have become more common in recent years. This has been aided by the development of longer-life batteries, charging via induction, and wireless connectivity.

Accurate measurement of the toe position can be used to prevent liner damage, and aids mill control and optimisation. This additional parameter can also be leveraged to calculate the total mill charge and ball charge. As mentioned previously, the Morrell C-model describes the geometry of the charge within its various sub-equations. One of these, Equation 5, relates total mill charge and mill speed to the toe position (Morrell, 1993), and thus, can be used to calculate the total mill charge if the toe position and mill speed are known.

$$\theta_T = 2.5307(1.2796 - J_t)(1 - e^{-19.42(\theta_c - \emptyset)}) + \frac{\pi}{2} \quad (5)$$

Where:

$J_t$  is the fractional mill filling.

$\theta_T$  is the angular displacement of the charge toe in radians based on the co-ordinate system outlined by Morrell (1993) and reproduced in Figure 7.

$\emptyset$  is the theoretical fraction of critical speed.

$\phi_c$  is the experimentally determined fraction of critical speed at which centrifuging was fully established in Morrell's test work. This was also found to be a function of mill filling ( $J_T$ ). When the mill is not near centrifuging conditions, the value of  $\phi_c$  is given by Equation 6.

$$\phi_c = 0.35(3.364 - J_t) \tag{6}$$

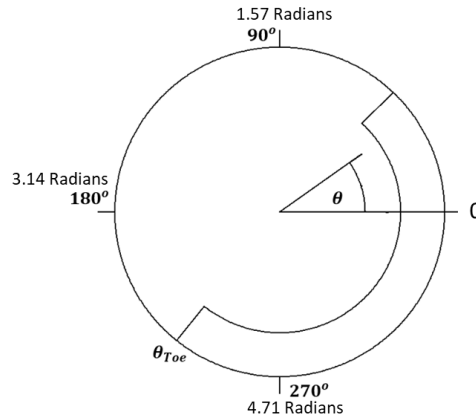


Figure 7—Morrell charge co-ordinate system (after Morrell, 1993)

Burns et al. (2018) present an industrial case study using toe measurement and the Morrell C-model to determine the total mill charge for the Lihir SAG mill. Due to the non-linearity of Equation 5, the mill charge could not be directly calculated from the toe position and had to be determined iteratively. However, analysis of Equation 5 and Morrell's (1993) original data (as shown in Figure 8) demonstrate that the toe location is only significantly affected by mill speeds when the speed is above 80% of theoretical critical speed (CS) or when the mill filling is above 40%. Most variable-speed drives do not go above 80% CS, and SAG mills typically operate at mill fillings below 40%. Therefore, Equation 5 can be simplified significantly to yield a linear equation (Equation 7). This in turn can be rearranged to give Equation 8, which provides a convenient linear relationship between a measured toe angle and calculated mill charge.

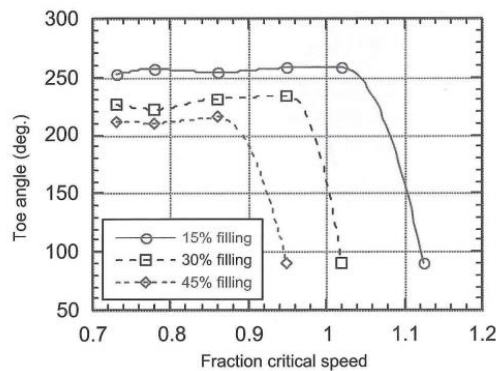


Figure 8—Morrell experimental results showing toe angle variation with mill charge and speed (Morrell, 1993)

$$\theta_T \cong 2.5307(1.2796 - J_t) + \frac{\pi}{2} \quad (7)$$

$$J_t \cong 1.2796 - \frac{\theta_T - \frac{\pi}{2}}{2.5307} \quad (8)$$

The difference between the mill charge calculated using the simplified version of the toe equation (Equation 8) and the full equation (Equation 5) for a range of different mill charge and speeds is shown in Table 1. The error increases with higher mill speeds and mill fillings but is less than 0.875% (absolute) provided the mill speed is less than 80% CS and mill filling is less than 40%, both of which are true for almost all SAG mills. For example, when the simplified Equation 8 predicts 35% total mill charge based on a toe measurement, and the mill speed is 75% CS, the full Morrell toe equation (Equation 5) would yield 35.249% mill charge. Therefore, the absolute difference (error) is only 0.249%. This small difference would be insignificant from a mill control or mill optimisation perspective. Using this modified equation (equation 8), large amounts of historian data can be assessed almost instantaneously with little accuracy sacrificed, thus enabling metallurgists to leverage all available data to measure, model, and optimise SAG mill performance.

Table 1—Absolute error from calculating mill charge from toe angle with Equation 8 versus Equation 5

		Mill Speed %Critical Speed					
		65%	70%	75%	80%	85%	90%
% Total Mill Charge	20%	0.015%	0.040%	0.104%	0.276%	0.728%	1.923%
	25%	0.020%	0.053%	0.140%	0.370%	0.976%	2.577%
	30%	0.027%	0.071%	0.187%	0.494%	1.304%	3.444%
	35%	0.036%	0.094%	0.249%	0.658%	1.738%	4.591%
	40%	0.048%	0.126%	0.331%	0.875%	2.311%	6.102%
	45%	0.063%	0.166%	0.439%	1.159%	3.061%	8.084%
	50%	0.083%	0.219%	0.580%	1.530%	4.041%	10.672%
	55%	0.109%	0.289%	0.762%	2.012%	5.313%	14.029%
	60%	0.143%	0.378%	0.997%	2.633%	6.952%	18.357%

Based on this analysis, the simplified linear relationship between toe measurement and total mill filling (Equation 8) provides a reasonable starting point for establishing a correlation between mill filling and toe angle for any SAG mill with a toe angle measurement. However, the predicted toe location is dependant on the signal (strain or vibration) used from the measurement device and how this signal is converted to a toe location. Therefore, we recommend that sites validate and calibrate this correlation for each mill using multiple measurements taken during crash-stops.

Burns et al. (2018) conducted four crash-stop inspections at Lihir and regressed total mill filling with the charge toe angle as predicted from the bolt sensor vibration and strain signal. Their regressed data are reproduced in Figure 9 and compared to the results from the simplified version of Morrell’s equation relating toe angle and mill charge (Equation 8). The toe angle predicted from the bolt sensor vibration data aligned well with the simplified Morrell relationship between mill charge and toe angle. Because the strain data are less sensitive and the predicted toe angle differed significantly from the vibration data and Morrell calculations, this output would require calibration to allow reporting of accurate mill filling values.

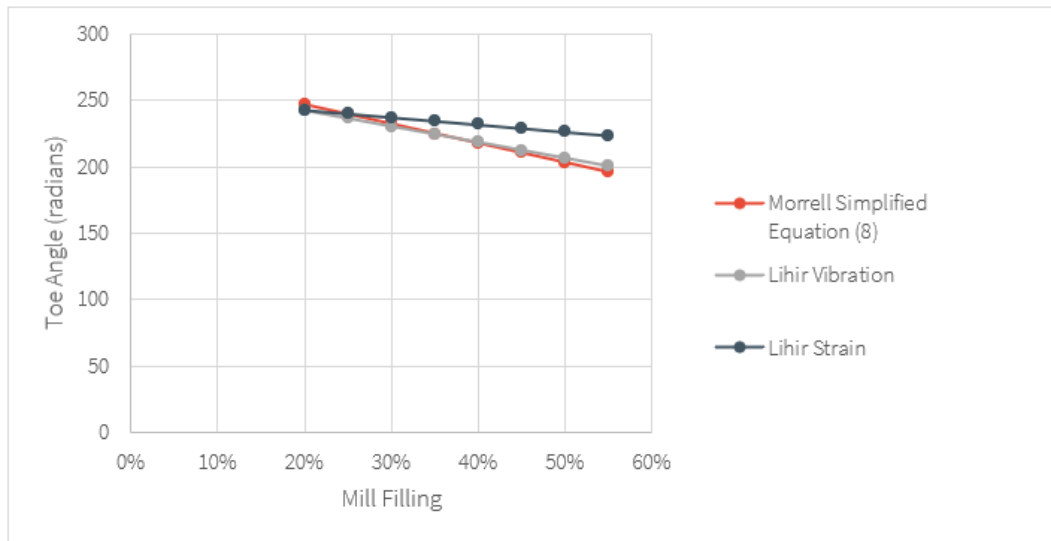


Figure 9—Comparison of toe angle measurement Vs morrell simplified toe equation (after Burns et al., 2018)

In addition to validating and calibrating the signal sensitivity used to predict toe angle, there is likely some dependence on the size distribution, rheology, and other factors of the mill charge which are unique to each mill and may result in some departure from Equation 8. This adds further justification for conducting multiple crash-stop inspections to calibrate the toe angle measurement and establishing a relationship to mill charge that is specific to that mill.

After having installed and conducted the appropriate verification and validation of the toe measurement device, the simplified calculation of mill filling is reasonably straightforward for large data sets. The ball charge can then be calculated using a power model.

The importance of calibrating the toe angle measuring device and conducting the subsequent verification and validation tests cannot be overstated. In the authors' experience many of the installed devices that report toe angle have not gone through a rigorous calibration and testing regime. In such scenarios, adopting the proposed methodology will result in erroneous mill fillings and ball loads being reported. Indeed, in such scenarios the proposed methodology may initially be used to conduct verification and validation of the measurement device.

As an example, toe angle measurement data were used to calculate total filling and ball filling using high-resolution (10 second intervals) historian data just prior to and during a grinding survey for a 36 ft SAG mill. During the survey, the mill was crash-stopped and ground-out, with the total filling and ball load measured at 24.4% and 15.5%, respectively.

A time-series trend of the period analysed is shown in Figure 10. The following observations are made:

- The toe angle measurement and subsequent calculated total mill filling trend is significantly affected by the change in mill speed at about 10:20 am. This results in an exaggerated reduction in mill filling from 40% to 30%, which does not correspond to the change in mill weight or the previous correlation in mill weight and mill filling.

- The erroneous step change in total filling results in a large step change in ball filling from approximately 9% to 13%, which is obviously incorrect given there was no addition of balls prior to the grinding survey.
- The calculated total filling was approximately 30%, and as previously mentioned the ball load was calculated at 13%. This differs greatly from the actual measured values. Using an offset (+C) of 8 degrees would bring the calculated value in line with the measured values; however, it is recommended that multiple measurements be taken to allow linear calibration in the form of  $mX+C$ .
- The calibration proposed above may aid in outputting more reliable measurements when the mill is in steady state. However, the analysis does show that the instrument is significantly affected by mill speed, and potentially other factors such as feed-size distribution. As such, in this case, the signal processing and filtering of the actual device measurements would need to be assessed.

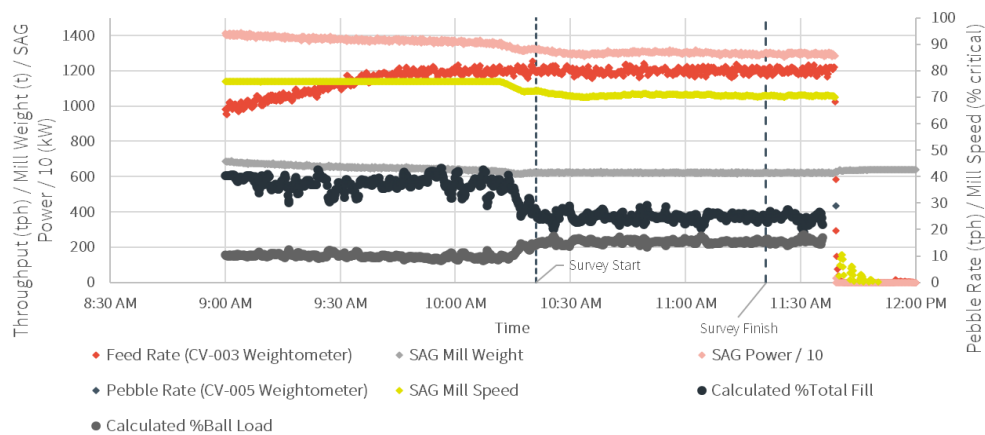


Figure 10—SAG mill trends with total mill charge and ball charge calculated using toe angle and power draw

As can be seen from this example, the method is mathematically possible, and outputs the desired parameters but is heavily predicated on the instrumentation having undergone proper calibration and testing at the time of installation and during subsequent upkeep. As suggested previously, the proposed methodology may act as initial check on the validity of the measurement, and after corrective action is taken may be used to calculate total mill filling and ball load.

### CASE STUDY 3: DETERMINING MILL CHARGE WITH LIFTER-LINER MODELS

Another method to determine the total mill volumetric charge (mill filling) and ball volumetric charge for a SAG mill is to use a power model in conjunction with a charge mass model (Aplet & Thornhill, 2009; Bird et al., 2012). For a given mill power draw there is a range of possible ball and total volumetric charges. However, there is a unique combination of ball charge and total charge for a given charge mass and power draw (Figure 11). For example, for a power draw of 21.5 megawatts (MW) the total volumetric charge could be 20% at a ball charge of 15%; it could also be 30% if the ball charge is 10%, or indeed other combinations. However, if the mass of the charge (ore + media + slurry) is known to be on the order of 700 tonnes this occurs when the mill charge is about 30% and ball charge is 10%. At a higher ball charge of 15%, the total mill charge is only 20%, and the mass of the charge is about 650 tonnes.

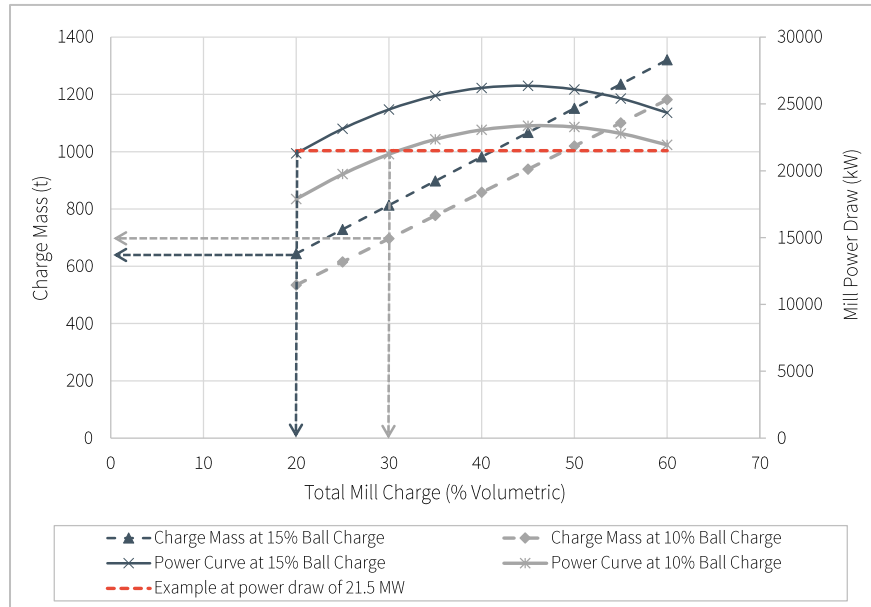


Figure 11—SAG mill power, charge mass, and mill charge relationships at 10% and 15% ball charge

The major difficulty with this approach is that the mill load reported to the control room is the total output given by load cells or bearing pressure rather than actual charge mass. These mill load measurements include the mill and liner weight, which itself is dynamic due to wear and mill relining. However, if the reported mill load could be adjusted to account for the changing liner mass, the charge mass could be determined, and the mill total and ball charges calculated using a power model.

The charge mass can be calculated (Equation 9) when the new liner mass is known from engineering drawings and the current liner mass could be derived from a wear model based on tonnes processed. The offset is incorporated to take the load reading from an unknown zero-load reference point to actual load for the mill with new liners and no charge in the mill.

$$Charge\ Mass = Load\ Reading + Offset + (New\ Liner\ Mass - Current\ Liner\ Mass) \quad (9)$$

Realistically, the only method able to develop a sufficiently accurate liner wear and liner weight model is one that uses the aid of laser scanning. This is now common procedure since Scanalyse introduced the MillMapper software in 2006 (Franke et al., 2006). An example of a liner-wear and liner-mass model based on laser scanning is shown in Figure 12. The liner-wear model also provides a method to update the mill internal diameter with respect to liner wear which can also have a significant impact on mill power draw (Toor et al., 2011).

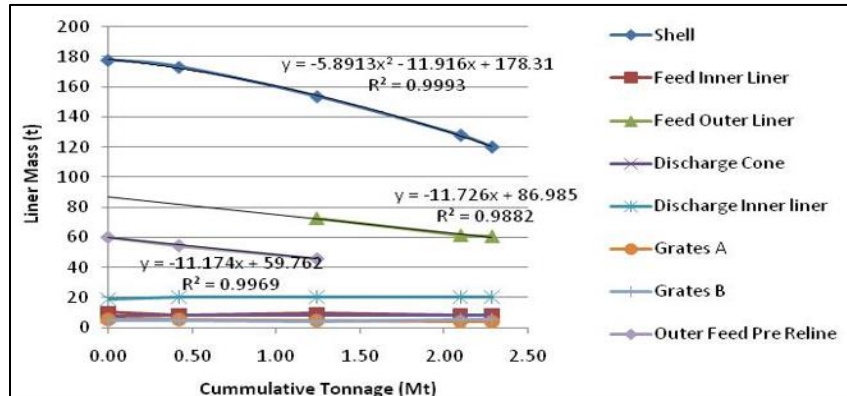


Figure 12—Example of measured lifter–liner mass loss from laser scanning

To use this approach, the slurry mass needs to be accounted for when determining the charge mass. Since the slurry occupies the charge voidage (assuming no slurry pooling) it can be represented as a fraction of the total charge volume, typically in the range of 0.7 to 1. The slurry fill fraction should be determined either by inspection or using semi-empirical relationships such as those Latchireddi and Morrell (2003a, 2003b) derived. Representing the slurry mass as a fraction of the total charge volume allows the charge mass to be represented in terms of ball and ore volume and total mass, as shown in Equation 10.

$$M_{Total} = V_{Ore} \times \rho_{Ore} \times (1 - \epsilon) + V_{Ball} \times \rho_{Ball} \times (1 - \epsilon) + (V_{Ore} + V_{Ball}) \times \rho_{Slurry} \times \text{slurry fill fraction} \times \epsilon \quad (10)$$

Where:

V is the volume (of ore and balls as indicated by subscripts).

$\rho$  is the density (of ore, balls and slurry as indicated by subscripts).

$\epsilon$  is the fractional porosity usually set to 0.4.

Equations 9 and 10 can be used in conjunction with a liner-wear model such as the one described in Figure 12 to calculate the ball and total charge using an algorithm (Figure 13). This can be set up and calculated using Excel.

A sensitivity analysis was conducted for the example mill with the wear measurements in Figure 14. This was conducted to evaluate the magnitude of error introduced from assuming a constant slurry fill fraction as well as any potential error in the liner wear and liner weight model. This sensitivity analysis is only relevant for the mill being assessed, and the sensitivity for other mills may vary because of different mill size, speed, charge levels, ore density, and so on. However, this provides an indication of the significance of the errors associated with these assumptions for this mill (a 40 ft, grate-discharge SAG mill).

For the example mill, changing the slurry fill fraction from 0.7 to 1.0 resulted in the total mill charge varying by approximately 0.5%, which is negligible, and within the acceptable range required for mill optimisation. The sensitivity to liner mass was more significant. A 10-tonne differential in liner mass resulted in the calculated mill charge varying by about 1% to 1.8%. A 10-tonne error in liner mass represents about 1.5% of the liner mass for the mill being assessed when new, and 5% of the total mass of the liners when in a worn state. This further confirms the requirement for accurate liner wear measurements via laser scanning. The sensitivity of liner mass on the calculated total and ball charge for this example is shown in Figure 14—Calculated ball and total charge sensitivity to liner weight Figure 14.



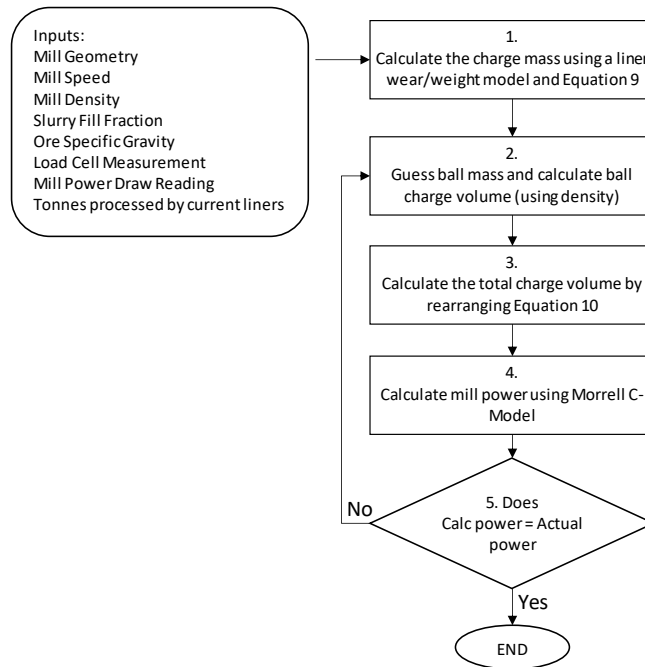


Figure 13—Algorithm for ball and total charge calculation using liner wear and liner weight model

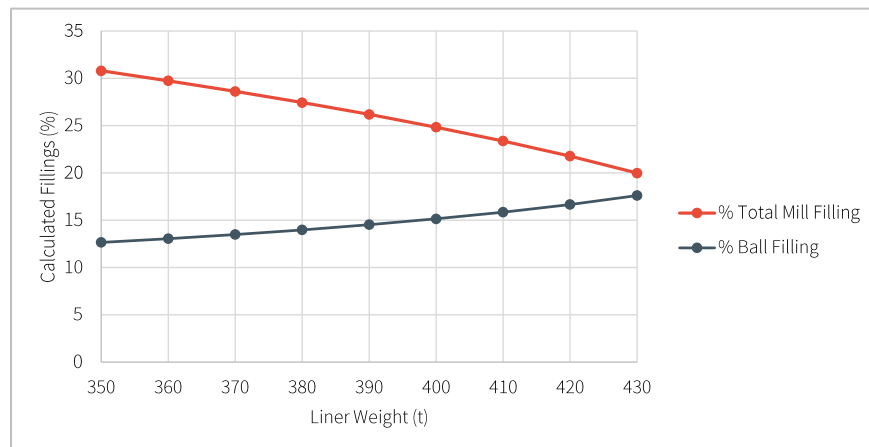


Figure 14—Calculated ball and total charge sensitivity to liner weight

## COMBINING METHODS TO DETERMINE MILL CHARGE

Three separate methods have been outlined to infer total mill charge for SAG mills using power modelling, with two of these methods also yielding the ball charge. These methods can be employed separately, but if two or more are employed in conjunction this would provide verification of the separate methods (Figure 15).

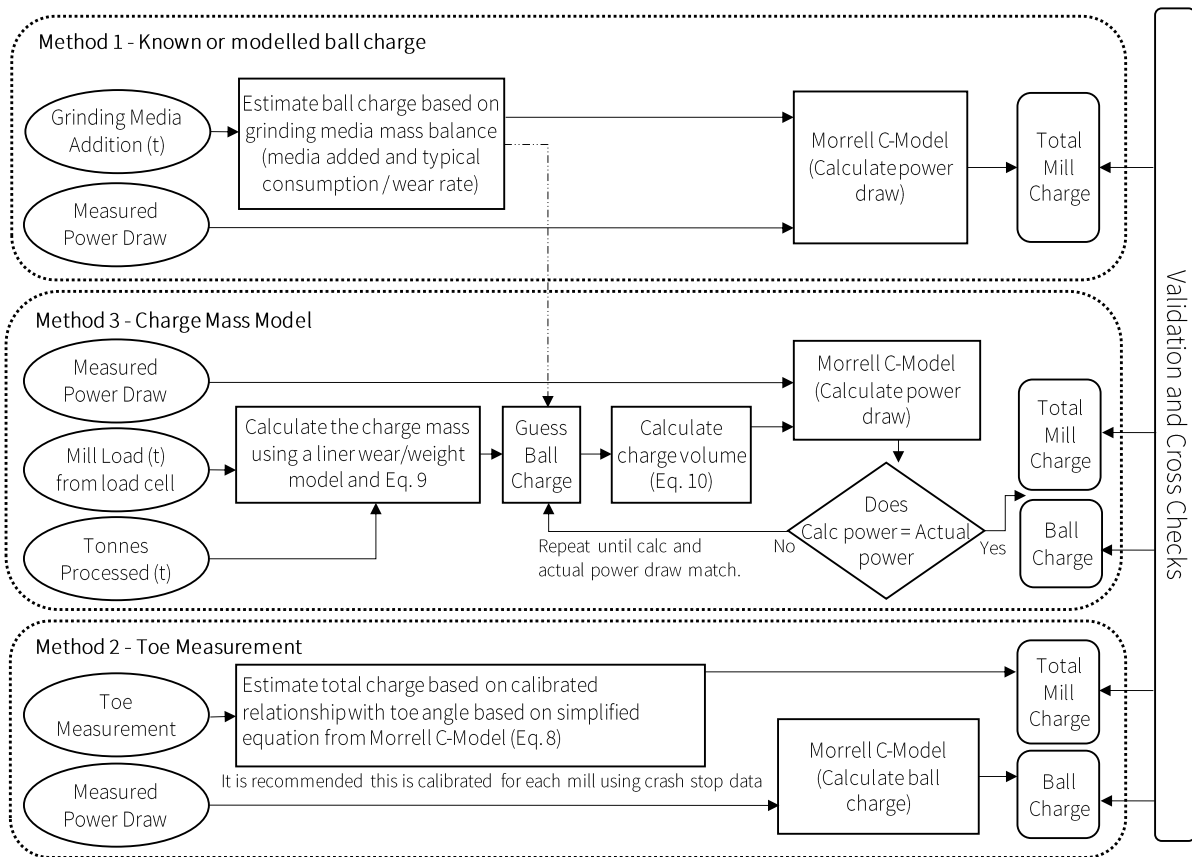


Figure 15—Combination of methods for verification

Each of the methods for calculating mill charge relies on assumptions, modelling, and measurements that can be erroneous. Using multiple methods provides a mechanism to verify the results by checking if they are consistent. Any discrepancies between values obtained provide an indication of an issue, such as poor calibration of toe measurement device, or potentially an early warning of abnormal lifter–liner wear. The proposed strategies should allow for better measurement, modelling, management, and ultimately optimization of SAG mills.

## Conclusion

SAG mill throughput and energy efficiency can be improved through optimizing total volumetric mill charge. If the mill filling is too low, this can decrease energy efficiency and increase liner wear; excessively high mill filling can reduce throughput and eventually result in mill overloading. However, measurements of mill load given by either load cells or bearing pressure also include mill and liner weight, which changes with wear. Therefore, it can be difficult to get a reliable measure of total mill filling without a crash-stop and inspection, which is generally conducted infrequently due to the production disruption.

Three methods have been described which allow mill filling to be calculated in real time and for large data sets, such as process historian data, thus enabling the results to be used for process optimization. The first method requires the ball charge to be known or modelled, but the other two methods allow calculation of total mill

charge and ball charge. However, these two methods require additional measurements (toe angle or laser scanning) and calibration of models and relationships for the mill. Nevertheless, once these relationships are established, the total and ball charge can be calculated with process historian data. Any one of these methods could be used, depending on the data and measurements available on site, or several could be used together to provide verification of results, as all include some assumptions and models which may introduce error.

Improved monitoring of total mill charge over time would allow identification of optimum operating conditions to improve SAG mill performance. This would also facilitate early detection of issues and aid in trouble-shooting and rectifying any issues.

## References

---

- Apelt, T., & Thornhill N. (2001). Inferential measurement of sag mill parameters. *Minerals Engineering* Vol 14(6):575-591.
- Bird, M., Powell, M.S., Hilden, M., (2011). Adapting mill control to account for liner wear on the Cadia 40 ft mill. *Proceedings International Autogenous and Semiautogenous Grinding Technology Conference 2011*, Vancouver, Canada.
- Burns, F., Aisthorpe, C., Blanz, P., Randall, M., Ebzery, P., (2018). Toe angle measurement for SAG mill control and Lihir Gold Mine. *Proceedings Mill Operators Conference 2018*, Brisbane, Australia.
- Doll, A. (2013). A comparison of SAG mill power models. *Proceedings Procemin 2013*, Santiago, Chile, 15-18 October.
- Franke, J., Lichti, D D., and Stewart, M P., (2006). MillMapper: A new tool for grinding mill thickness gauging, *Proceedings International Autogenous and Semiautogenous Grinding Technology 2006*, Vancouver, Canada
- Global Mining Guidelines Group. (2021). The Morrell Method to Determine the Efficiency of Industrial Grinding Circuits. Website: <https://gmgroup.org/guidelines-and-publications/morrell-method-to-determine-the-efficiency-of-industrial-grinding-circuits/>
- Hart, S., Valery Jnr., W., Clements, B., Reed, M., Ming Song, Dunne, R. (2001) Optimisation of the Cadia Hill SAG Mill Circuit. SAG2001 - SAG mill circuit. *International Conference on Autogenous and Semiautogenous Grinding Technology 2001*, Vancouver, Canada
- Latchireddi, S. and Morrell, S. (2003a). Slurry flow in mills: grate-only discharge mechanism (Part1). *Minerals Engineering*, 16 (7): 625-633.
- Latchireddi, S. and Morrell, S. (2003b). Slurry flow in mills: grate-pulp lifter discharge systems (Part 2). *Minerals Engineering*, 16 (7): 635-642.
- Lawson, V, Carr, D, Valery Jr, Burford B, Pease, J, and Man, Y (2001) Evolution and optimisation of the copper concentrator autogenous grinding practices at mount isa mines limited *Proceedings International Autogenous and Semiautogenous Grinding Technology Conference 2001*, Vancouver, Canada.
- Morrell, S. (1993). The prediction of power draw in wet tumbling mills. (Doctoral Dissertation), University of Queensland, Australia.
- Morrell, S. (1996a). Power draw of wet tumbling mills and its relationship to charge dynamics - Part 1: A continuum approach to mathematical modelling of mill power draw. *Transactions of the Institutions of Mining and Metallurgy, Section C: Mineral Processing and Extractive Metallurgy*. 105. C43-C51.
- Morrell, S. (1996b). Power draw of wet tumbling mills and its relationship to charge dynamics - Part 2: An empirical approach to modelling of mill power draw. *Transactions of the Institutions of Mining and Metallurgy, Section C: Mineral Processing and Extractive Metallurgy*. 105. C54-C59.
- Morrell, S. (2003). Grinding mills: how to accurately predict their power draw. *Proceedings XXII International Mineral Processing Congress (pp. 55-99)*. Cape Town, South Africa.
- Morrell, S. (n.d.). *Session 6 - Tumbling Mill Power Draw Modelling*, SMC Masterclass series on comminution by SMC Testing. Retrieved on July 24, 2023,

Napier-Munn, T., Morrell, S., Morrison, R., & Kojovic, T. (1996). *Mineral Comminution Circuits - Their Operation and Optimisation*. Brisbane: Julius Kruttschnitt Mineral Research Centre.

S. Strohmayr, W. Valery Jr. (2001) SAG mill circuit optimisation at ernest henry mining *Proceedings International Autogenous and Semiautogenous Grinding Technology Conference 2001*, Vancouver, Canada

Toor, P, Franke, J, Powell, M S and Perkins, T, (2011). Quantifying the influence of liner shape and mill filling for performance optimization, *Proceedings International Autogenous and Semiautogenous Grinding Technology Conference 2011*, Vancouver, Canada.

## Appendix A—Morrell C-Model Calculations

---

See previous nomenclature provided in the introduction to Morrell C-model section. Full details of the model and its derivation can be found in the JKMRM monograph, Mineral Comminution Circuits (Napier-Munn, Morrell, Morrison, & Kojovic, 1996) and is also well described with all equations and a worked example in Morrell, 1996a.

### Step 1 Calculate charge density ( $\rho_c$ )

$$\rho_c = \frac{J_t \rho_o (1 - E + EUS) + J_B (\rho_B - \rho_o) (1 - E) + J_t EU (1 - S)}{J_t}$$

### Step 2 Calculate toe angle, slurry toe angle and shoulder angle

2a Calculate Fraction of theoretical critical speed at which centrifuging actually occurs ( $\phi_c$ )

$$\phi_c = \phi; \text{ if } \phi > 0.35(3.364 - J_t)$$

$$\phi_c = 0.35(3.364 - J_t); \text{ if } \phi \leq 0.35(3.364 - J_t)$$

2b Calculate toe angle in radians ( $\theta_T$ )

$$\theta_T = 2.5307(1.2796 - J_t)(1 - e^{-19.42(\phi_c - \phi)}) + \frac{\pi}{2}$$

2c Calculate slurry toe angle in radians ( $\theta_{TO}$ )

$$\text{For grate discharge mill } \theta_{TO} = \theta_T$$

$$\text{For overflow discharge mill } \theta_{TO} = \pi + \arcsin\left(\frac{r_t}{r_m}\right)$$

Note, the overflow discharge relationship can also be used for slurry pooling, in which case  $r_t$  is the radius to the surface of the slurry pool (rather than the trommel radius).

2d Calculate shoulder angle in radians ( $\theta_S$ )

$$\theta_S = \frac{\pi}{2} - \left(\theta_T - \frac{\pi}{2}\right) \times [(0.3386 + 0.1041\phi) + (1.54 - 2.5673\phi)J_t]$$

### Step 3 Calculate inner surface radius of charge

3a Calculate mean rotational rate ( $N_{mean}$ )

$$N_{mean} = \frac{N_m}{2}$$

3b Calculate mean radial position ( $r_{mean}$ )

$$r_{mean} = \frac{r_m}{2} \left[ 1 + \left( 1 - \frac{2\pi J_t}{2\pi + \theta_S - \theta_T} \right)^{0.5} \right]$$

3c Calculate time to travel from toe to shoulder in active charge ( $t_c$ )

$$t_c = \frac{2\pi - \theta_T + \theta_S}{2\pi N_{mean}}$$

3d Calculate time to travel from shoulder to toe in free flight ( $t_f$ )

$$t_f = \left( \frac{2r_{mean}(\sin\theta_S - \sin\theta_T)}{g} \right)^{0.5}$$

3e Calculate fraction of total charge in active region ( $\beta$ )

$$\beta = \frac{t_c}{t_f + t_c}$$

3f Calculate radial location of inner surface of charge ( $r_i$ )

$$r_i = r_m \left( 1 - \frac{2\pi\beta J_t}{2\pi + \theta_S - \theta_T} \right)^{0.5}$$

#### Step 4 Calculate z parameter

$$z = (1 - J_t)^{0.4532}$$

#### Step 5 Calculate power draw due to motion of charge

5a Calculate charge motion power in the cylindrical section ( $P_t$ )

$$P_t = \frac{\pi g L N_m r_m}{3(r_m - z r_i)} [2r_m^3 - 3z r_m^2 r_i + r_i^3 (3z - 2)] \times [\rho_c (\sin\theta_S - \sin\theta_T) + \rho_p (\sin\theta_T - \sin\theta_{T0})] + L \rho_c \left( \frac{N_m r_m \pi}{(r_m - z r_i)} \right)^3 [(r_m - z r_i)^4 - r_i^4 (z - 1)^4]$$

5b Calculate charge motion power in conical section ( $P_c$ )

$$P_c = \frac{\pi L_d g N_m}{3(r_m - r_i)} \left\{ (r_m^4 - 4r_m r_i^3 + 3r_i^4) \times [\rho_c (\sin\theta_S - \sin\theta_T) + \rho_p (\sin\theta_T - \sin\theta_{T0})] \right\} + \left( \frac{2\pi^3 N_m^3 L_d \rho_c}{5(r_m - r_i)} \right) (r_m^5 - 5r_m r_i^4 + 4r_i^5)$$

5c Calculate total charge motion power draw ( $P_{charge\ motion}$ )

$$P_{charge\ motion} = P_t + P_c$$

**Step 6 Calculate no-load power ( $P_{no-load}$ )**

$$P_{no-load} = K_2 \times D^{2.05} [\phi(0.667L_d + L)]^{0.82}$$

$K_2 = 1.68$  for gear and pinion drives

$K_2 = 1$  for gearless drives

**Step 7 Calculate gross power ( $P_{gross}$ )**

$$P_{gross} = P_{no-load} + k \times (P_{charge\ motion})$$

$k = 1.26$